Quantized Ionic Conductance in Nanopores

Michael Zwolak,[1] Johan Lagerqvist,[2] and Massimiliano Di Ventra[2]

[1]*Theoretical Division, MS-B213, Los Alamos National Laboratory, Los Alamos, New Mexico 87545, USA*
[2]*Department of Physics, University of California, San Diego, La Jolla, California 92093, USA*

(Received 13 April 2009; published 17 September 2009)

Ionic transport in nanopores is a fundamentally and technologically important problem in view of its occurrence in biological processes and its impact on novel DNA sequencing applications. Using molecular dynamics simulations we show that ion transport may exhibit strong nonlinearities as a function of the pore radius reminiscent of the conductance quantization steps as a function of the transverse cross section of quantum point contacts. In the present case, however, conductance steps originate from the break up of the hydration layers that form around ions in aqueous solution. We discuss this phenomenon and the conditions under which it should be experimentally observable.

DOI: 10.1103/PhysRevLett.103.128102 PACS numbers: 87.16.Vy

Over the last decade there have been tremendous advances in both the fabrication of nanopores and their use for molecular recognition and nucleic acid analysis [1]. Experimental characterization of molecules has mostly relied on measuring changes in the ionic current through the pore [2–5], but other ways to probe single molecules in nanopores may come from embedding nanoscale sensors within the pore or nanochannels [6–9]. Irrespective, electronic fluctuations due to the dynamical ionic and aqueous environment affect the type of signals and noise these sensors detect. Therefore, understanding the electrostatics of ions in water at atomic length scales is crucial to our ability to design functional single-molecule sensors and to interpret their output, and will also provide new insight into the operation of biological ion channels.

Several studies have examined the electrostatics of ions in nanopores using continuum dielectric models for water [10–12]. Within a continuum model, the nanopore electrostatic environment is essentially one dimensional due to the large difference of dielectric constants between water and the pore [11]. Thus, according to these models, there is a large electrostatic energy penalty to move an ion from the exterior of the pore to its interior [10,11], with small amounts of surface charge able to drastically reduce this energy penalty [10]. Although continuum models can highlight some generic features of ionic currents and blockades, such as the effect of surface charges, they miss important effects related to the microscopic physical structure of water molecules around ions.

In this Letter, we examine ionic transport from the point of view of these nanoscale features (see schematic in Fig. 1). Using all-atom molecular dynamics simulations, we calculate the structural and electrostatic details of a single ion in an aqueous environment both in and out of cylindrical nanopores of different radii. Ions in solution create local structures in the surrounding water, known as *hydration layers* [13], and characterized by oscillations in the water density. The length scales associated with these oscillations and their decay are in the range ~2–10 Å, i.e., comparable to the radial dimensions of some nanopores. We show that when the ion is inside the pore, water molecules form wavelike features due to both the interaction with the walls and the water molecules in the partially broken hydration layers. Based on these microscopic observations, we predict that the ionic conductance of a nanopore manifests steplike features as a function of the pore radius, similar to the quantized conductance of quantum point contacts as a function of their effective cross section (see, e.g., [14]). Finally, we examine the influence of noise and discuss the experimental conditions under which the above steplike features should be observable.

To be specific, we focus on an isolated chlorine anion but similar considerations apply to other ions and situations. We perform molecular dynamics simulations to obtain the structural details of the ion inside and outside cylindrical Si_3N_4 nanopores of 100 Å depth and different radii. The simulation details are as in Ref. [7]. For all simulations, a single Cl^- is taken as fixed since its thermal wavelength at room temperature is ~0.2 Å. In the immediate vicinity of the Cl^-, the water molecules orient themselves so that a single hydrogen from each molecule points inward toward the ion (see Fig. 1). The distribution of

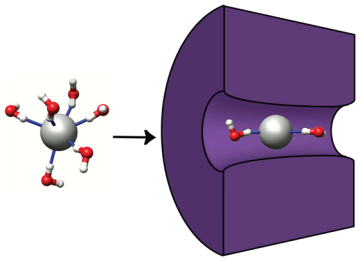

FIG. 1 (color online). Schematic of a single anion with its first hydration layer moving into a nanopore. Because of spatial constraints, water molecules need to be stripped off from the ion, creating nonlinearities in the ionic conductance.

water molecules forms into layers as shown in Fig. 2 [15]. The inner most layer is very tightly bound, and subsequent layers are spaced at 2.0–2.3 Å. These findings are in good agreement with neutron diffraction and x-ray absorption experiments that measure the radial distribution of water [16], which give a Cl-O peak at ~3.1 Å, as well as molecular dynamics simulations performed with different force field parameters [17]. In addition, we can acquire further information not directly accessible from experiments, such as the microscopic electric field due to the ions and water [shown in the inset of Fig. 2(b)]. This field shows oscillations corresponding to the hydration layers and is similar to a series of alternating charged surfaces. A continuum picture would not capture these microscopic details that are responsible for the conductance steps we predict.

If the anion is now placed in the nanopore, the hydration layers are affected. For instance, in Figs. 2(c) and 2(d), one observes wavelike features that are due to interference patterns between oscillations reflecting off the walls of the pore (that set an effective pore radius) and those around the ion. These patterns depend on pore size—different pore sizes can give maxima and minima in the water density along the pore axis. Further, we find that when the effective pore radius is ~3 Å there is a transition in the water structure in the pore [18]. Irrespective, for large pores, the hydration layer structure is identical to that in bulk water. As the pore is taken to nanoscale dimensions, eventually the pore walls force the hydration layers to be partially broken because they can not fit within the pore; see Figs. 2(c) and 2(d). Within a 15 Å radius pore, the first

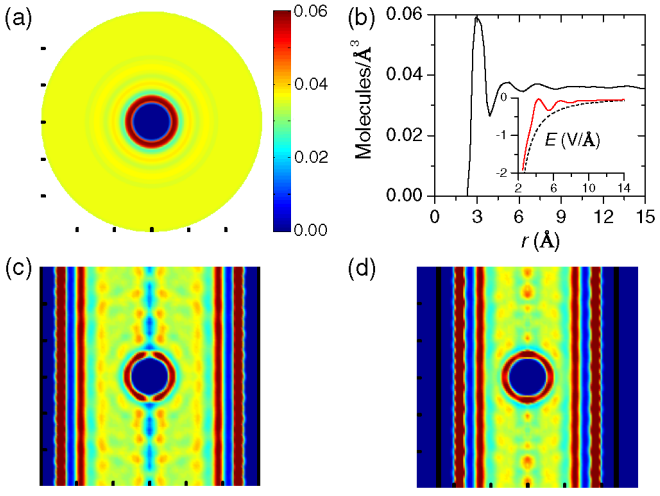

FIG. 2 (color online). (a) Water density around Cl^- in bulk. (b) Water density versus radial distance from Cl^-. The inset shows the time-averaged radial electric field (versus the radial distance) from both the ion and water dipoles (red line) and from just the ion (black dashed line). Water density around Cl^- inside a (c) 15 Å radius pore and (d) 12 Å radius pore. The pore walls are indicated by vertical, thick black lines. However, the effective radius R_p is smaller, as can be seen from the figure.

and second hydration layers are still present. On the other hand, for a 12 Å radius, the first layer is intact, but the second layer is partially broken by the effective pore wall. In other words, only the portion of the layers along the axis of the pore remain intact.

In view of these numerical results, we propose the following model system for uniform diameter pores that captures this essential aspect of the presence of hydration layers around the ion. We consider a set of surfaces placed at each hydration layer, i, at radius R_i. Each surface represents the area where the water dipoles fluctuate, giving the time-averaged dipole layers. Ignaczak *et al.* [19] have found that for small water clusters around a Cl^-, the internal energy of each water is approximately linear in the number of water molecules in the cluster. Since interactions (van der Waals and electrostatic) with a low dielectric pore are small compared to water-ion and water-water interactions [20], we write the internal energy contained in a partially intact hydration layer as $U_i = f_i U_i^0$, where f_i is the fraction of the layer present in the pore and U_i^0 is the energy difference of the intact water layer and the water in bulk.

In this model, the energy barrier is due to the stripping off of a fraction of the layer, f_i, i.e., the fraction of a spherical surface at R_i remaining in the pore of effective radius R_p. When the ion translocates along the pore axis, the surface area that remains in layer i is given by

$$S_i = 2\Theta(R_i - R_p) \int_0^{2\pi} d\phi \int_0^{\theta_c} d\theta R_i^2 \sin\theta, \qquad (1)$$

where $\Theta(x)$ is the step function and $\theta_c = \sin^{-1} R_p/R_i$. When $R_p < R_i$, the fraction of the surface left is

$$f_i(R_p) = 1 - \sqrt{1 - \left(\frac{R_p}{R_i}\right)^2}. \qquad (2)$$

The internal energy barrier as a function of pore radius is then given by $\Delta U(R_p) = \sum_i (f_i(R_p) - 1) U_i^0$, where the summation is over the layers. The free energy change of hydration is dominated by the contribution from the total internal energy contained within the hydration layers, $\sum_i U_i^0$, plus a bulk dielectric contribution from water outside the layers. Previous calculations give the total internal energy change in the range -3.5 to -3.7 eV [19,21]. The form of the electric field shown in Fig. 2(b) suggests that the time-averaged microscopic distribution of waters can be viewed as a set of spherical layers of alternating charge. Thus, the energy stored within each layer is well estimated by using a Born solvation calculation, which, by construction, sums to the total internal energy contribution. This corresponds to summing the energy of "quasiparticles." For example, the energy of the first layer is the difference of solvating the ion and solvating the ion plus the first layer, i.e., solvating a quasiparticle consisting of the ion and a cluster of waters. With this picture in mind, the energy within each layer is given by

$$U_i^0 = \frac{e^2}{8\pi\epsilon_0}\left(1 - \frac{1}{\kappa}\right)\left(\frac{1}{R_i^O} - \frac{1}{R_i^I}\right), \quad (3)$$

where κ is the water dielectric constant and $R_i^{I(O)}$ are the inner (outer) radii demarcating the hydration layer, and we have used the effective ion charge of $1e$, since the field nearly recovers its bare ion value after each hydration layer [see Fig. 2(b)]. From the water density oscillations shown in Fig. 2, these radii are 2.0 and 3.9 Å for the first layer, 3.9 and 6.2 Å for the second, 6.2 and 8.5 Å for the third. The total solvation energy is then -3.6 eV and the layer energies are -1.7, -0.7, and -0.3 eV for the first, second, and third layers, respectively. Immediately, we can understand why the third layer is absent within these pores: entropic contributions from the water structure and van der Waals interactions are of the same magnitude.

In addition to the internal energy change, there is also an entropic contribution to the free energy change that comes from removing a single ion from solution and localizing it in the pore. Assuming an ideal ionic solution, this entropic contribution is $\Delta S = k_B \ln(V_p n_0)$, where V_p is the volume of the pore, n_0 is the bulk salt concentration, and k_B is the Boltzmann constant. The final free energy difference, $\Delta F = \Delta U - T\Delta S$, is plotted in Fig. 3. This is the main result of this work: hydration layers hold energy in a shell-like structure that causes steplike features in the energy barrier to ionic transport. These steplike features generate corresponding features in the current. The latter can be estimated from $I = 2\pi R_p^2 e\mu n E$, where μ is the ion mobility, E is the strength of the electric field, and $n = n_0 \exp(-\Delta F/kT)$ is the pore salt concentration. This latter expression for the concentration recognizes that any feature in the free energy change of ions will result in a corresponding feature in the ionic current due to the suppression of the concentration within the pore. This current is plotted in Fig. 3.

For the remainder of this Letter, we discuss the conditions under which these features should be observable experimentally and address how the assumptions we have made affect our conclusions. First, we have assumed that only the single ion barrier is important, i.e., that there are no correlated transport processes. This is valid only in the absence of significant surface charges within the pore and at low bulk concentrations. Without surface charges, the energetic barrier creates a very low concentration of ions in the pore (see, e.g., Ref. [22]), which suppresses the ability of current-carrying ions and counterions to correlate their motion through the pore. Likewise, a low bulk concentration and a small applied bias is necessary for well-defined hydration layers to exist, and also to limit the concentration of ions in the pore. Bulk ion concentrations below 1 M are therefore necessary [23]. Also, for all layers to be present, the applied bias has to be sufficiently small as to not generate fields of the order $\sim$0.1 V/Å (the electric field in the vicinity of the third layer) and thus not significantly disturb the hydration layer structure. On the other hand, the

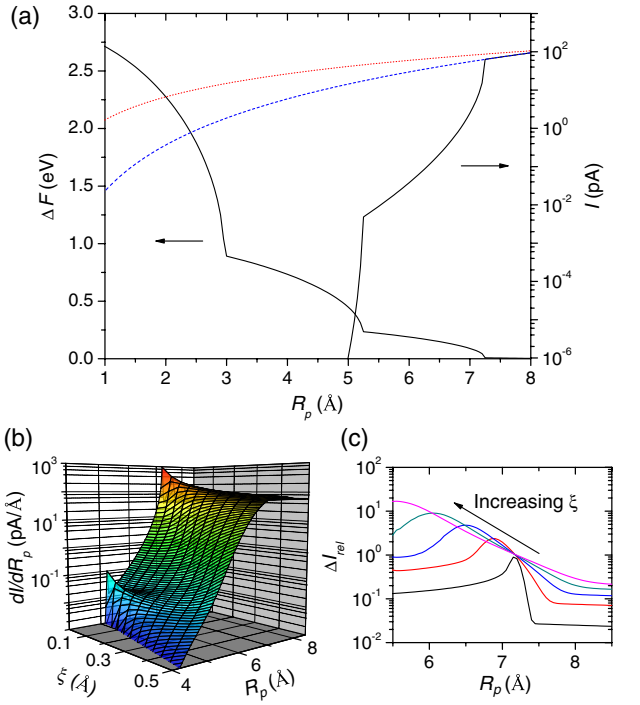

FIG. 3 (color online). (a) Free energy barrier to bring an ion into a nanopore and the ionic current at room temperature as a function of the effective pore radius R_p. The current is for a field of 1.2 mV/Å, and 1 M bulk salt concentration, assuming a typical ion mobility of $\mu = 2.28 \times 10^{-8}$ m^2/V s [25]. The dotted red line indicates the ionic current without a free energy barrier and the dashed blue line is the current with just the entropic barrier. (b) dI/dR_p as a function of pore radius and noise strength ξ. For zero noise, the steplike features in the ionic current give rise to well-defined peaks in the derivative of the current. However, as the noise is increased, the peaks smooth out. (c) Relative noise, $\Delta I_{\rm rel} = (\langle I^2\rangle - \langle I\rangle^2)^{1/2}/\langle I\rangle$, versus pore radius for the outermost hydration layer and for $\xi = 0.05$, 0.15, 0.25, 0.35, 0.45 Å.

ionic concentration itself may be used to observe the steplike features. Namely, at certain concentrations the anion-anion (cation-cation) distance would be small enough so that the hydration layers should break with increasing concentration, resulting in a nonlinearity in the current. Second, we have neglected energetic fluctuations due to other effects, such as thermal noise, ion-ion interaction, rough pore surfaces, a distribution of ion paths through the pore, and the fact that hydration layers are not exactly represented by their time-averaged oscillations (therefore, some ions with intact hydration layers could go into pores smaller than the radius R_i would predict). In order to determine how robust the steplike features are to these noise sources, we have added in our calculations Gaussian noise in the pore radius. In particular, we define a noise strength parameter ξ (i.e., the standard deviation of the Gaussian noise) to describe both energetic and path fluctuations. In Fig. 3, we plot dI/dR_p as a function of R_p and ξ. For no noise, $\xi = 0$ Å, there are well-defined peaks in dI/dR_p. However, at a noise strength of $\xi = 0.2$–0.3 Å,

the peaks from the second and third layers are smoothed out. Given the width of the hydration layers as seen in Fig. 2, the effects from the second and third layers may not be observable when transport is due to ions like Cl^-, or K^+. However, other ions, such as the divalent Mg or trivalent Al ions, as well as some monovalent ions, have more strongly bound second and third layers. Together with using tunable properties, such as temperature, this may allow observation of the steplike features in the current. In addition, the noise gives an alternative way to observe the effect of the hydration layers. As shown in Fig. 3(c), the relative noise peaks when the pore radius is near that of a hydration layer. This effect can be understood in terms of a two-state picture: fluctuations that decrease the pore radius energetically ''close'' the pore, whereas fluctuations that increase the pore radius ''open'' it, essentially creating an instability in the current. Such an effect could also be induced artificially by sampling over a distribution of pore radii centered around a layer radius. Finally, a strong affinity of the ions for the pore wall may occur, for instance, if the pore were significantly charged. This effect may indeed reduce the energy barrier for ionic transport considerably, making all but the first hydration layer breakup undetectable in the ionic current. The charging of the pore walls, which depends heavily on pore material and treatment, as well as other factors, can again be somewhat resolved by observing transport with different ion and pore types.

To conclude, we have predicted that ionic transport in nanopores should show steplike features as a function of pore radius due to the presence of hydration layers. This effect is the classical counterpart of the electronic quantized conductance one observes in quantum point contacts as a function of their cross section. Like the quantum case, one needs sufficient experimental control of the nanopore characteristics in order to observe this effect. Irrespective, a drop in the current should be observable when the first hydration layer is reached, similar to what is thought to occur in the open and closed states of some biological pores [24]. Experiments with more well-controlled synthetic pores, of which nanotube pores may be particularly suitable, will help shed light on the different factors at work. We hope our results will help understand and motivate experiments that specifically examine the role of dehydration in ionic transport.

This research is supported by the NIH-NHGRI (J. L. and M. D.) and by the U. S. Department of Energy through the LANL/LDRD Program (M. Z.).

[1] M. Zwolak and M. Di Ventra, Rev. Mod. Phys. **80**, 141 (2008).
[2] J. J. Kasianowicz, E. Brandin, D. Branton, and D. W. Deamer, Proc. Natl. Acad. Sci. U.S.A. **93**, 13 770 (1996).
[3] M. Akeson, D. Branton, J. J. Kasianowicz, E. Brandin, and D. W. Deamer, Biophys. J. **77**, 3227 (1999).
[4] A. Meller, L. Nivon, E. Brandin, J. Golovchenko, and D. Branton, Proc. Natl. Acad. Sci. U.S.A. **97**, 1079 (2000).
[5] W. Vercoutere, S. Winters-Hilt, H. Olsen, D. Deamer, D. Haussler, and M. Akeson, Nat. Biotechnol. **19**, 248 (2001).
[6] M. Zwolak and M. Di Ventra, Nano Lett. **5**, 421 (2005).
[7] J. Lagerqvist, M. Zwolak, and M. Di Ventra, Nano Lett. **6**, 779 (2006); Biophys. J. **93**, 2384 (2007); Phys. Rev. E **76**, 013901 (2007).
[8] J. B. Heng, A. Aksimentiev, C. Ho, V. Dimitrov, T. W. Sorsch, J. F. Miner, W. M. Mansfield, K. Schulten, and G. Timp, Bell Labs Tech. J. **10**, 5 (2005); M. E. Gracheva, A. Xiong, A. Aksimentiev, K. Schulten, G. Timp, and J.-P. Leburton, Nanotechnology **17**, 622 (2006); M. E. Gracheva, A. Aksimentiev, and J.-P. Leburton, Nanotechnology **17**, 3160 (2006).
[9] X. Liang and S. Y. Chou, Nano Lett. **8**, 1472 (2008).
[10] J. Zhang, A. Kamenev, and B. I. Shklovskii, Phys. Rev. Lett. **95**, 148101 (2005); A. Kamenev, J. Zhang, A. Larkin, and B. Shklovskii, Physica (Amsterdam) **359A**, 129 (2006).
[11] S. Teber, J. Stat. Mech. (2005) P07001.
[12] D. Jan Bonthuis, J. Zhang, B. Hornblower, J. Mathe, B. I. Shklovskii, and A. Meller, Phys. Rev. Lett. **97**, 128104 (2006).
[13] B. Hille, *Ion Channels of Excitable Membranes* (Sinauer Associates, Sunderland, 2001).
[14] M. Di Ventra, *Electrical Transport in Nanoscale Systems* (Cambridge University Press, Cambridge, England, 2008).
[15] The plots for an ion in a spherical water droplet are averages of the last 900 of 1000 snapshots (taken at 1 ps intervals) within spherical shells of thickness 1 Å. For an ion inside a pore, the last 4000 out of 5000 snapshots (taken at 0.1 ps intervals) are averaged within cylindrical shells of thickness 1 Å in both the radial and vertical directions. The pore surfaces carry a charge of $6–8 \times 10^{-4}\ e/\text{atom}$. The electric field is calculated by averaging the ion and dipole moment contributions.
[16] H. Ohtaki and T. Radnai, Chem. Rev. **93**, 1157 (1993).
[17] Z. Z. Yang and X. Li, J. Phys. Chem. A **109**, 3517 (2005).
[18] G. Hummer, J. C. Rasaiah, and J. P. Noworyta, Nature (London) **414**, 188 (2001).
[19] A. Ignaczak, J. A. N. F. Gomes, and M. N. D. S. Cordeiro, Electrochim. Acta **45**, 659 (1999).
[20] L. Yang and S. Garde, J. Chem. Phys. **126**, 084706 (2007).
[21] J. Chandrasekhar, D. C. Spellmeyer, and W. L. Jorgensen, J. Am. Chem. Soc. **106**, 903 (1984).
[22] S. Joseph, R. J. Mashl, E. Jakobsson, and N. R. Aluru, Nano Lett. **3**, 1399 (2003).
[23] A typical ion (counting both anions and cations) is contained in a volume with linear dimension 9.4 Å for a 1 M bulk salt concentration. This is large enough to almost house both the first and second hydration layers. For arbitrary concentrations, the ion-ion distance goes as $\sim 9.4/n_0^{1/3}$ Å, where n_0 is in mols/L. To allow all hydration layers to be present, one would want a concentration of ~ 0.1 M.
[24] C. Peter and G. Hummer, Biophys. J. **89**, 2222 (2005).
[25] D. W. Deamer and D. Branton, Acc. Chem. Res. **35**, 817 (2002).